



저작자표시-비영리-변경금지 2.0 대한민국

이용자는 아래의 조건을 따르는 경우에 한하여 자유롭게

- 이 저작물을 복제, 배포, 전송, 전시, 공연 및 방송할 수 있습니다.

다음과 같은 조건을 따라야 합니다:



저작자표시. 귀하는 원저작자를 표시하여야 합니다.



비영리. 귀하는 이 저작물을 영리 목적으로 이용할 수 없습니다.



변경금지. 귀하는 이 저작물을 개작, 변형 또는 가공할 수 없습니다.

- 귀하는, 이 저작물의 재이용이나 배포의 경우, 이 저작물에 적용된 이용허락조건을 명확하게 나타내어야 합니다.
- 저작권자로부터 별도의 허가를 받으면 이러한 조건들은 적용되지 않습니다.

저작권법에 따른 이용자의 권리는 위의 내용에 의하여 영향을 받지 않습니다.

이것은 [이용허락규약\(Legal Code\)](#)을 이해하기 쉽게 요약한 것입니다.

[Disclaimer](#)

2022년 2월  
박사학위논문

# Estimation of Groundwater Level based on Kriging Techniques

조선대학교 대학원

자연과학과(수학전공)

정 나 영

# Estimation of Groundwater Level based on Kriging Techniques

크리깅 기법에 의한 지하수 수위의 추론

2022년 2월 25일

조선대학교 대학원

자연과학과(수학전공)

정 나 영

# Estimation of Groundwater Level based on Kriging Techniques

지도교수    강   성   권

이 논문을 이학박사학위신청 논문으로 제출함

2021년 10월

조선대학교 대학원

자연과학과(수학전공)

정   나   영

## 정나영의박사학위논문을인준함

심사위원장 조선대학교 교수 정 윤 태 인

심사위원 조선대학교 교수 김 남 권 인

심사위원 조선대학교 교수 김 광 섭 인

심사위원 전남대학교 교수 진 홍 성 인

심사위원 조선대학교 교수 강 성 권 인

2022년 1월

조선대학교 대학원

# C O N T E N T S

## 국문 초록

1. Introduction	1
2. Semivariogram and mathematical models	3
3. Nonlinear parameter estimation	5
4. Kriging	8
5. Application	12
5.1. Spatial ratio and anisotropy	12
5.2. Averaging process	13
5.3. Examples	14
5.3.1. Example 1	14
5.3.2. Example 2	24
6. Conclusion	39
References	40

## 국 문 초 록

### 크리깅 기법에 의한 지하수 수위의 추론

정 나 영

지도교수 : 강 성 권

조선대학교 대학원  
자연과학과(수학전공)

강 하구의 퇴적 대수층에서 수집된 지하수 수위에 대한 제한된 데이터를 바탕으로, 대수층 구성 물질의 분포 상태가 연속이라는 가정하에 측정되지 않은 지점에서의 수위를 추론하고, 그 지역의 지하수 흐름의 방향을 추론하였다. 현장 데이터에 내재 되어 있는 불확실성을 연속적 평균 개념, 공간적 비율, 방향성 등을 응용하여 상관관계를 계산하고, 그 상관관계를 나타내는 수학적 모델(선형, 비선형)은 매개변수 추론 기법을 이용하여 찾았으며, 그 모델들을 크리깅 체계에 적용하여 샘플 지역의 지하수 흐름 방향 등을 추론하였다.

이 논문에서 고려된 개념들과 최적화 기법들은 측정되지 않은 지점에서의 지하수 수위를 잘 추론하였다. 제안된 개념과 방법들은 연속성을 갖는 퇴적 대수층에서의 지하수 흐름 방향 등을 추론하는데 활용될 수 있다.

## 1. Introduction

Kriging was introduced by a mining engineer Krige for estimating the distribution of mining materials [12]. Since then many geostatistical methods related to Kriging have been developed and applied to various area such as mining materials, groundwater contaminants, environmental protections, groundwaters, etc [21, 22].

The theories on Geostatistics related to hydrology and spatial data have been studied for many years [2, 8, 9, 11, 15, 17]. The Macro Dipersion Experiments (MADE 2) were performed the experimental site , experiments, and related data are explained in, for example, [1, 3, 4, 5, 6, 14, 19, 20].

Kriging process involves several optimization problems such as parameter estimations for linear or nonlinear models representing the semivariograms showing the correlation between sample distances and their values. Theory and practical techniques for optimization, we refer [10, 13, 16, 18].

In this paper, Kriging techniques are applied to estimate groundwater levels at unmeasured locations. Based on the in-situ measured groundwater level samples, kriging system together with the conceptions such as overlapping averaging process, spatial ratio, direction are applied for finding appropriate experimental semivariograms. To estimate the parameters appearing in mathematical semivariogram models such as polynomials, exponentials, spherical [8], linear or nonlinear optimization techniques are applied. In particular, for the nonlinear parameter estimations, a real version of Complex Nonlinear Parameter Estimation (CNPE) together with a robust optimization algorithm [13] can be used. The CNPE with its robust algorithm has been developed for handling highly nonlinear and severely ill-posed problems. Two sample data sets, water tables, adopted in this paper, were chosen from the MADE-2 experiments [1, 3, 5, 6, 19, 20]. The region collected samples is an alluvial aquifer. One set consisted of 26 water tables was used for analysis in [7]. In [7], the kriging with,



for example, non-overlapping averaging and drift were applied to reform the optimization procedures. Collected near the first sample site, the other samples were for investigating hydraulic conductivities. The numerical estimation results with various conceptions show improvement of experimental semivariograms representing the correlation between  $lag\ h$  and groundwater levels compared with those by conventional kriging methods. Those conception and optimization kriging system can be applied for continuous alluvial aquifer.

In Section 2, semivariograms and mathematical models for regionalized variables are explained. Kriging is introduced in Section 3. Section 4 considers a real version of CNPE with a robust optimization algorithm. The implimentation of continued averaging process, spatial ratio, anisotropies in kriging system are explained in Section 5. The estimation results including the groundwater flow direction in the test site are shown in this section. Conclusions are in Section 6.

## 2. Semivariogram and mathematical models

As one of the basic statistical measures of geostatistics, the semivariogram represents the variance of a regionalized variable with respect to a certain distance *lag* [17]. A regionalized variable such as ore material distributed under the ground or water table is a realization of a random variable [15].

Let  $Z(X)$  be a regionalized variable at a location  $X$  in a region  $\Omega$ . Let

$$\{Z(X_i) | X_i \in \Omega, 1 \leq i \leq n\} \quad (2.1)$$

be a set of samples measured at location  $X_i$ ,  $1 \leq i \leq n$ . The *semivariogram* (or *experimental semivariogram*) to a lag  $h$  is defined by

$$\gamma(h) = \frac{1}{2N(h)} \sum_{i=1}^{N(h)} |Z(X_i) - Z(X_i + h)|^2, \quad (2.2)$$

where  $N(h)$  is the number of data pairs separated by the vector  $h$  [8]. In many practical regionalized variables the semivariogram (2.2) shows erratic behaviors so that a certain averaging process may be needed for producing an appropriate correlation between the lag and the corresponding variance.

To obtain a continuous information from a discrete experimental semivariogram, mathematical models can be considered. The spherical model

$$\gamma(h) = \begin{cases} c_0 + \beta \left( \frac{3h}{2\alpha} - \frac{h^3}{2\alpha^3} \right), & h \leq \alpha, \\ c_0 + \beta, & h > \alpha, \end{cases} \quad (2.3)$$

the exponential model

$$\gamma(h) = c_0 + c_1 \left( 1 - \exp \left( -\frac{h}{c_2} \right) \right) \quad (2.4)$$

and the linear or cubic polynomial

$$\gamma(h) = c_0 + ah \quad (2.5)$$

$$\gamma(h) = c_0 + ah + bh^2 + ch^3 \quad (2.6)$$

may be considered depending on the distribution profile of semivariogram [8, 9]. Here,  $h = \|\mathbf{h}\|$  is the radius of the vector  $\mathbf{h}$ , and the parameter  $c_0$  is the nugget effect,  $c_0 + \beta$  is the *sill* value.

**Remark 2.1.** (i) Mathematical models (2.3)-(2.6) are functions of the radius  $h$ , i.e.,  $\gamma(h)$  depends on the distance between sample locations not on the individual location.  
(ii) Since the mathematical models are continuous functions for any lag  $h$ ,  $\gamma(h)$  can be calculated.  
(iii) To obtain the parameters appeared in the mathematical models, a certain optimization technique may be needed.

### 3. Nonlinear parameter estimation

In this section, we consider a real version of the complex nonlinear parameter estimation (CNPE) [13].

Let

$$F : \mathbb{R}^M \rightarrow \mathbb{R}^N \quad (3.1)$$

be the nonlinear operator from a parameter space to a sample space, where  $\mathbb{R}^M$  is the  $M$ -dimensional parameter space and  $\mathbb{R}^N$  is the  $N$ -dimensional sample space. More precisely,

$$F(\beta) = [F_1(\beta), F_2(\beta), \dots, F_N(\beta)]^T, \quad (3.2)$$

$$\beta = [\beta_1, \beta_2, \dots, \beta_M]^T \in \mathbb{R}^M, \quad (3.3)$$

where  $F$  is the  $N$ -dimensional nonlinear operator and  $\beta$  is the  $M$ -dimensional parameter vector.  $F$  can be a mathematical model or differential equation.

**Optimization problem[OP] :** For any sample data

$$Y = [y_1, y_2, \dots, y_N]^T \in \mathbb{R}^N, \quad (3.4)$$

find a best parameter  $\beta^* = [\beta_1^*, \beta_2^*, \dots, \beta_M^*]^T \in \mathbb{R}^M$  minimizing the cost

$$S(\beta) = \sum_{i=1}^N |y_i - F_i(\beta)|^2. \quad (3.5)$$

For a given parameter  $\beta$ , to obtain an increment parameter  $\delta = [\delta_1, \delta_2, \dots, \delta_M]^T \in \mathbb{R}^M$ , we linearize  $S(\beta + \delta)$  at  $\beta$ .

$$S(\beta + \delta) = \sum_{i=1}^N |y_i - F_i(\beta + \delta)|^2 \approx \sum_{i=1}^N \left| y_i - \left( F_i(\beta) + \frac{\partial F_i}{\partial \delta}(\beta) \delta \right) \right|^2, \quad (3.6)$$

where

$$\frac{\partial F_i}{\partial \delta}(\beta) = \left[ \frac{\partial F_i}{\partial \delta_1}(\beta), \frac{\partial F_i}{\partial \delta_2}(\beta), \dots, \frac{\partial F_i}{\partial \delta_M}(\beta) \right]. \quad (3.7)$$

**Remark 3.1.** If  $F$  or  $F_i$  is in the form of differential equation, it is not easy to find the sensitivity of  $F_i$  with respect to  $\delta_j$ , i.e.,  $\frac{\partial F_i}{\partial \delta_j}$ . In such cases, we may replace  $\frac{\partial F_i}{\partial \delta_j}$  by  $\frac{F_i(\delta_j + \epsilon) - F_i(\delta_j)}{\epsilon}$  for a small positive  $\epsilon > 0$ .

Let

$$J(\beta) = [J_1(\beta), J_2(\beta), \dots, J_N(\beta)]^T, \quad J_i(\beta) = [J_{i1}(\beta), J_{i2}(\beta), \dots, J_{iM}(\beta)], \quad (3.8)$$

where

$$J_{im}(\beta) = \frac{\partial F_i}{\partial \delta_m}(\beta), \quad 1 \leq i \leq N, \quad 1 \leq m \leq M. \quad (3.9)$$

In terms of matrix,

$$J(\beta) = \begin{bmatrix} \frac{\partial F_1}{\partial \delta_1}(\beta) & \frac{\partial F_1}{\partial \delta_2}(\beta) & \cdots & \frac{\partial F_1}{\partial \delta_M}(\beta) \\ \frac{\partial F_2}{\partial \delta_1}(\beta) & \frac{\partial F_2}{\partial \delta_2}(\beta) & \cdots & \frac{\partial F_2}{\partial \delta_M}(\beta) \\ \vdots & \vdots & \ddots & \vdots \\ \frac{\partial F_N}{\partial \delta_1}(\beta) & \frac{\partial F_N}{\partial \delta_2}(\beta) & \cdots & \frac{\partial F_N}{\partial \delta_M}(\beta) \end{bmatrix},$$

the normal equations become

$$\frac{\partial S(\beta + \delta)}{\partial \delta_j} = 0, \quad 1 \leq j \leq M. \quad (3.10)$$

After some manipulation, the equations (3.10) become

$$[J(\beta)]^T [J(\beta)] \delta = [J(\beta)]^T (Y - F(\beta)). \quad (3.11)$$

**Remark 3.2.**[13] (i) Equation (3.11) is the solution formula for the linearized version of the optimization problem (OP).

(ii) The formula (3.11) is the necessary condition for the increment  $\delta$  to be satisfied for a local minimum of  $S(\beta + \delta)$ . Thus,

$$S(\beta + \delta) < S(\beta). \quad (3.12)$$

(iii)  $\frac{\partial S(\beta + \delta)}{\partial \delta_j} = 0$ ,  $1 \leq j \leq M$  in (3.10) represent the sensitivities of the cost  $S$  with respect to the parameter  $\delta$ .

(iv) The *Jacobian*  $J(\beta)$  in (3.11) is  $N \times M$  matrix so that  $[J(\beta)]^T[J(\beta)]$  is  $M \times M$  matrix.

(v) Sometimes, the square matrix  $[J(\beta)]^T[J(\beta)]$  may be singular so that the formula (3.11) might not be solved for  $S$ . For such cases, we consider a *regularization parameter*  $\rho$  such that the regularized system

$$([J(\beta)]^T[J(\beta)] + \rho I) \delta = [J(\beta)]^T(Y - F(\beta)) \quad (3.13)$$

to be solved. In many cases,  $\rho = 0.001$  can be used.

To solve the regularized system (3.13), we consider the following robust algorithm.

**Algorithm 3.3.**[13] Step 1. Choose initial guesses for the parameter vector  $\beta$  and the regularization parameter  $\rho > 0$ .

Step 2. Compute the cost  $S(\beta)$  in (3.5).

Step 3. Compute  $J(\beta)$  in (3.8)-(3.9) and solve the linear system (3.13) for  $\delta$ . Calculate  $S(\beta + \delta)$ .

Step 4. If  $S(\beta + \delta) < S(\beta)$ , update  $\beta$  by  $\beta + \delta$  and  $\rho$  by, for example,  $\frac{\rho}{10}$ . Go to Step 2.

Step 5. If the criterion  $S(\beta + \delta) < S(\beta)$  is failed, update  $\rho$  by, for example,  $10\rho$  and repeat Step 3 until the criterion is satisfied.

Step 6. Continue Step2-Step5 until the cost  $S(\beta)$  in (3.5) reaches a minimum.

**Remark 3.4.** Algorithm 3.3 is a robust optimization algorithm. It is designed for treating severely ill-posed problems. The algorithm moves from a Newton type to a Steepest descent scheme and vice versa.

## 4. Kriging

Kriging is an interpolation method to estimate values at unmeasured locations for regionalized variables. Kriging uses information from the semivariogram to find an optimal set of weights. For more information, see [12].

The kriging is based on the geostatistical assumption.

- 1)  $E[Z(X)] = E[Z(X + \mathbf{h})]$ .
- 2) For any vector  $\mathbf{h}$  the increment  $[Z(X) - Z(X + \mathbf{h})]$  has a finite variance which does not depend on  $X$ .

Let  $Z^*(X_0)$  be the value estimated at an unmeasured location  $X_0$ , and be consisted of a linear combination of the selected sample values,

$$Z^*(X_0) = \sum_{i=1}^n \omega_i Z(X_i), \quad (4.1)$$

where  $\omega_i$ 's are weights to be determined. Consider the following two constraints

$$E[Z^*(X_0) - Z(X_0)] = 0,$$

$$E[\{Z^*(X_0) - Z(X_0)\}^2] \text{ is a minimum with respect to } \omega_i, \quad (4.2)$$

where  $Z(X_0)$  is the value of the random function  $Z$  at  $X_0$ . These constraints mean that the difference  $Z^*(X_0) - Z(X_0)$  is *unbiased* and the variance of this difference is a minimum. From (4.1) and (4.2) we have

$$E \left[ \sum_{i=1}^n \omega_i Z(X_i) - Z(X_0) \right] = 0. \quad (4.3)$$

Let  $m$  be the unknown constant mean of the expectation. Then,

$$\sum_{i=1}^n \omega_i E[Z(X_i)] - E[Z(X_0)] = \sum_{i=1}^n \omega_i m - m = 0$$

and, thus

$$\sum_{i=1}^n \omega_i = 1. \quad (4.4)$$

Consider the following *Lagrange function* [18].

$$L(\omega_1, \omega_2, \dots, \omega_n; \lambda) = E \left[ \left[ \sum_{i=1}^n \omega_i Z(X_i) - Z(X_0) \right]^2 \right] - 2\lambda \left( \sum_{i=1}^n \omega_i - 1 \right), \quad (4.5)$$

where  $\omega_1, \omega_2, \dots, \omega_n$  are weights,  $\lambda$  is the *Lagrange multiplier*. The kriging problem becomes the following.

**Kriging problem[KP]** : Find  $\omega_1, \omega_2, \dots, \omega_n$ , and  $\lambda$  that minimize  $L(\omega_1, \omega_2, \dots, \omega_n; \lambda)$  in (4.5).

We consider the kriging problem mentioned above and the semivariogram defined in Section 2.

We derive a simplified form for Lagrange function (4.5) in the following. The simplified form can be written in terms of a matrix-vector form

$$\left[ \sum_{i=1}^n \omega_i Z(X_i) - Z(X_0) \right]^2 = \left( \sum_{i=1}^n \omega_i Z(X_i) \right)^2 - 2 \sum_{i=1}^n \omega_i Z(X_i) Z(X_0) + Z(X_0)^2. \quad (4.6)$$

Since

$$\begin{aligned} \left( \sum_{i=1}^n \omega_i Z(X_i) \right)^2 &= \sum_{i=1}^n \sum_{j=1}^n \omega_i \omega_j Z(X_i) Z(X_j) \\ &= \sum_{i=1}^n \sum_{j=1}^n \omega_i \omega_j \frac{-(Z(X_i) - Z(X_j))^2 + Z(X_i)^2 + Z(X_j)^2}{2} \\ &= - \sum_{i=1}^n \sum_{j=1}^n \omega_i \omega_j \frac{(Z(X_i) - Z(X_j))^2}{2} + \sum_{i=1}^n \sum_{j=1}^n \frac{\omega_i \omega_j Z(X_i)^2 + \omega_i \omega_j Z(X_j)^2}{2} \\ &= - \sum_{i=1}^n \sum_{j=1}^n \omega_i \omega_j \frac{(Z(X_i) - Z(X_j))^2}{2} + \sum_{i=1}^n \omega_i \frac{Z(X_i)^2}{2} + \sum_{j=1}^n \omega_j \frac{Z(X_j)^2}{2} \\ &= - \sum_{i=1}^n \sum_{j=1}^n \omega_i \omega_j \frac{(Z(X_i) - Z(X_j))^2}{2} + \sum_{i=1}^n \omega_i Z(X_i)^2. \end{aligned}$$



(4.6) becomes

$$\begin{aligned}
 \left[ \sum_{i=1}^n \omega_i Z(X_i) - Z(X_0) \right]^2 &= - \sum_{i=1}^n \sum_{j=1}^n \omega_i \omega_j \frac{(Z(X_i) - Z(X_j))^2}{2} \\
 &\quad + \sum_{i=1}^n \omega_i Z(X_i)^2 - 2 \sum_{i=1}^n \omega_i Z(X_i) Z(X_0) + \sum_{i=1}^n \omega_i Z(X_0)^2 \\
 &= - \sum_{i=1}^n \sum_{j=1}^n \omega_i \omega_j \frac{(Z(X_i) - Z(X_j))^2}{2} + 2 \sum_{i=1}^n \omega_i \frac{(Z(X_i) - Z(X_0))^2}{2}.
 \end{aligned} \tag{4.7}$$

Therefore, the Lagrange function defined in (4.5) becomes

$$\begin{aligned}
 &L(\omega_1, \omega_2, \dots, \omega_n; \lambda) \\
 &= - \sum_{i=1}^n \sum_{j=1}^n \omega_i \omega_j \gamma(X_i - X_j) + 2 \sum_{i=1}^n \omega_i \gamma(X_0 - X_i) - 2\lambda \left( \sum_{i=1}^n \omega_i - 1 \right),
 \end{aligned} \tag{4.8}$$

where  $\gamma$  is the semivariogram. By differentiating  $L(\omega_1, \omega_2, \dots, \omega_n; \lambda)$  in (4.8) with respect to  $\omega_1, \omega_2, \dots, \omega_n, \lambda$ , we have the following two conditions

$$-2 \sum_{j=1}^n \omega_j \gamma(X_i - X_j) + 2\gamma(X_0 - X_i) - 2\lambda = 0, \quad i = 1, 2, \dots, n \tag{4.9}$$

$$\sum_{i=1}^n \omega_i = 1. \tag{4.10}$$

The system (4.9) with the constraint (4.10) becomes the following equation in terms of matrix form

$$AW = B \tag{4.11}$$

where

$$A = \begin{bmatrix}
 \gamma(X_1 - X_1) & \gamma(X_1 - X_2) & \cdots & \gamma(X_1 - X_n) & 1 \\
 \gamma(X_2 - X_1) & \gamma(X_2 - X_2) & \cdots & \gamma(X_2 - X_n) & 1 \\
 \vdots & \vdots & \ddots & \vdots & \vdots \\
 \gamma(X_n - X_1) & \gamma(X_n - X_2) & \cdots & \gamma(X_n - X_n) & 1 \\
 1 & 1 & \cdots & 1 & 0
 \end{bmatrix},$$

$$W = [\omega_1, \omega_2, \dots, \omega_n, \lambda]^T,$$

$$B = [\gamma(X_0 - X_1), \gamma(X_0 - X_2), \dots, \gamma(X_0 - X_n), 1]^T.$$

**Remark 4.1.** (i)  $A$  is a  $(n + 1) \times (n + 1)$  symmetric matrix. The optimal weights  $\omega_1, \omega_2, \dots, \omega_n$  and the Lagrange multiplier  $\lambda$  can be obtained from  $W = A^{-1}B$ .

(ii) The resulting estimation variance of the kriging becomes

$$\sigma^2 = \sum_{i=1}^n \omega_i \gamma(X_0 - X_i) + \lambda - \gamma(X_0 - X_0). \quad (4.12)$$

## 5. Application

In this section, a continuous averaging process, spatial ratio and anisotropies such as spatial directions are explained. Two in situ sample sets are adopted for application. We apply the kriging techniques to a sample data set collected during a field experiment [4, 6, 14, 20]. All computations were performed on a personal computer, and the algorithms needed for our analyses were developed under the MATLAB environment.

### 5.1. Spatial ratio and anisotropy

Spatial ratio and directions are to account for anisotropic effects due to different range of influence on different directions in data distribution. Those are realization of advection and dispersion or diffusion processes of groundwater in conjunction with aquifer materials. The ratio may be obtained by comparing the data range in different directions. The directional consideration may be needed for accounting apparent directional tendencies.

## 5.2. Averaging process

The aquifer of a given site may be consisted of various materials so that the aquifer shows heterogeneity [8, 11, 15]. In particular, the experimental semivariograms show erratic behaviors in many cases. To obtain a continuous information of the semivariogram, the averaging process can be considered. Two kinds of averaging process may be considered, i.e., a certain size of spatial averaging and a fixed number of measured samples. Many sampling networks are performed on irregularly spaced locations. Moreover, the cost for sampling increased as the sample size becomes large so that the number of samples can be small. Thus, for those cases, we prefer to consider the regional averaging. More specifically, we consider the following strategy.

Let  $d$  be a lag average radius. Let  $M$  be the number of equal divisions for the interval  $[h_{min}, h_{max}]$  and  $H, H', h_{min}, h_{max}, dh$  be

$$H = \{ \|X_i - X_j\| : i < j, 1 \leq i, j \leq N \},$$

$$h_{min} = \min \{ h \in H \}, \quad h_{max} = \max \{ h \in H \}, \quad dh = \frac{h_{max} - h_{min}}{M},$$

$$H' = \{ h_{min}, h_{min} + dh, h_{min} + 2dh, \dots, h_{max} \}$$

$$= \{ h'_1, h'_2, h'_3, \dots, h'_{M+1} \}$$

Let  $I_1, I_2, \dots, I_{M+1}$  be

$$I_1 = \left\{ h_l \in H : |h'_1 - h_l| < d, \quad 1 \leq l \leq \frac{N(N-1)}{2} \right\} \text{ for } h'_1,$$

$$I_2 = \left\{ h_l \in H : |h'_2 - h_l| < d, \quad 1 \leq l \leq \frac{N(N-1)}{2} \right\} \text{ for } h'_2,$$

$$\vdots$$

$$I_{M+1} = \left\{ h_l \in H : |h'_{M+1} - h_l| < d, \quad 1 \leq l \leq \frac{N(N-1)}{2} \right\} \text{ for } h'_{M+1}.$$

The semivariogram after averaging process becomes

$$[ \text{mean}\{\gamma(I_1)\}, \text{mean}\{\gamma(I_2)\}, \dots, \text{mean}\{\gamma(I_{M+1})\} ].$$

### 5.3. Examples

#### 5.3.1. Example 1

The data set selected for our analyses consists of 26 groundwater level elevations measured in the deep level of the test site aquifer. The aquifer at the test site consists of a shallow alluvial terrace deposit averaging approximately 11m in thickness. The aquifer is composed of poorly-sorted to well-sorted sandy gravel and gravelly sand with minor amounts of silt and clay. Sediments are generally unconsolidated, and occur as irregular horizontal or nearly horizontal lenses and layers. Marine sediments belong to the Eutaw Formation and consisting of clays, silts, and fine-grained sands form an aquitard beneath this alluvial aquifer [7]. More details on the test site and other related previous experiments, see [1, 3, 5, 6, 19, 20]. The estimations are performed under the assumption that the test site can be extended continuously to a larger region.

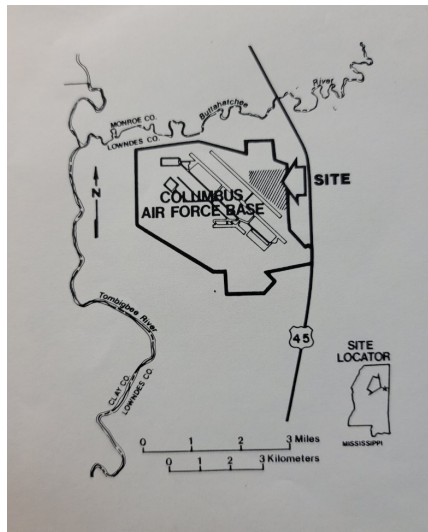


Figure 1: Test site location, Columbus AFB, MS

Figure 1 shows the test site location, Columbus Air Force Base, Mississippi.

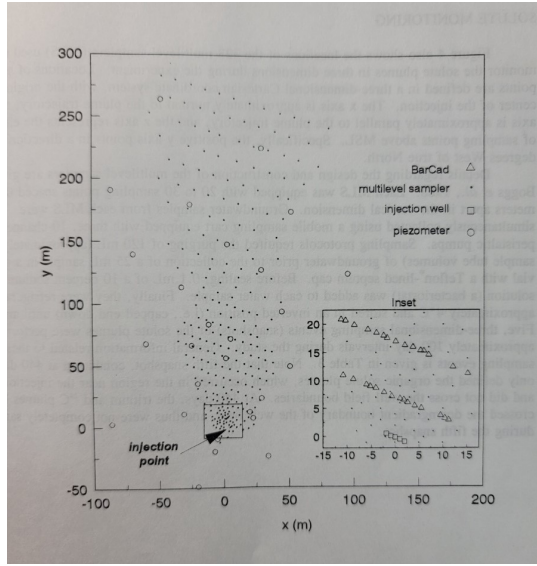


Figure 2: Sample site for Example 1

Figure 2 shows the sample site for Example 1. The positive y axis points in a direction 12 degrees West of true North. Thus the positive x axis points in a direction 12 degrees North of true East. The circles in Figure 2 show the well locations for Example 1. This site was designed for experiment of transport and biodegradation of some organic chemicals [6].

Table 1: Water levels for Example 1

Sample	$x(m)$	$y(m)$	$w(m)$	Sample	$x(m)$	$y(m)$	$w(m)$
P-1	-86.1	2.56	64.89	P-14	43.33	94.53	64.74
P-2	-11.41	83.28	64.53	P-15	-59.8	67.92	64.75
P-3	1.62	56.17	64.68	P-16	52.2	47.77	64.87
P-4	-30.84	10.38	64.71	P-17	-4.92	-10.33	65.14
P-5	-85.85	190.51	64.13	P-18	-20.13	35.08	64.77
P-6	95.13	123.75	64.79	P-19	29.26	22.95	64.82

Sample	$x(m)$	$y(m)$	$w(m)$	Sample	$x(m)$	$y(m)$	$w(m)$
P-7	103.2	5.73	65.82	P-20	-32.26	113.18	64.58
P-8	-19.4	-50.16	65.29	P-21	29.24	127.12	64.67
P-9	22.61	6.42	64.92	P-22	-69.15	139.66	64.57
P-10	-23.3	66.57	64.28	P-23	-25.7	179.32	64.59
P-11	3.16	147.63	64.59	P-24	29.34	225.1	64.46
P-12	32.44	-25.81	65.1	P-25	-47.8	263.96	64.13
P-13	5.55	71.69	64.75	P-26	51.93	173.77	64.59

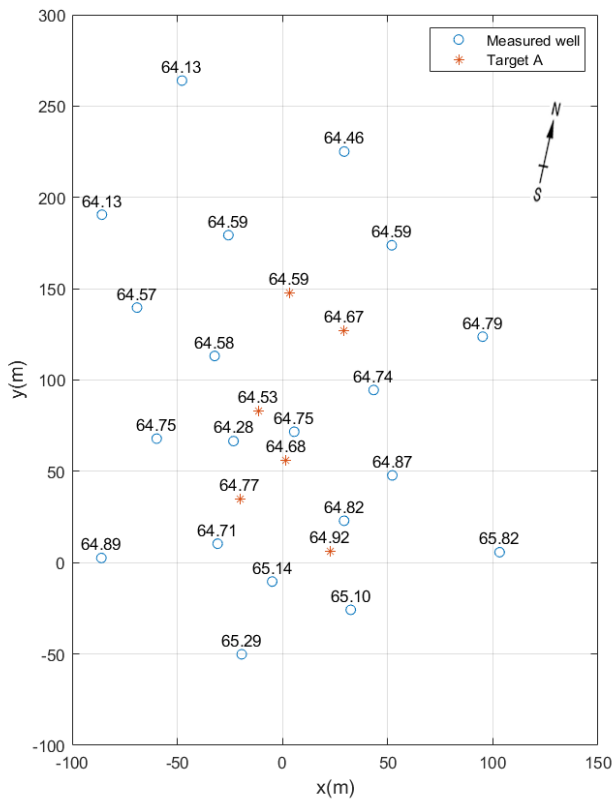


Figure 3: Water levels and Target A

Table 1 shows the 26 samples with location and water level elevation in meter scale. We selected six samples, Target A, arbitrarily from the inside of the convex domain consisted of the given 26 samples. Estimating Target A is an interpolation problem. Target A is shown in Figure 3.

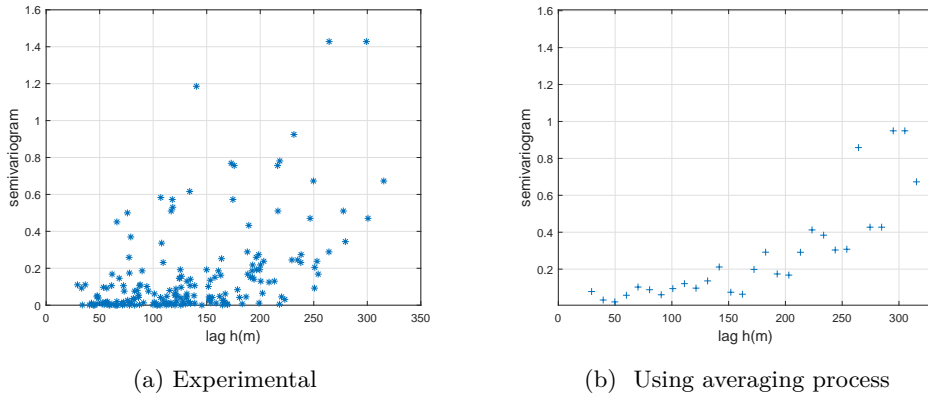


Figure 4: Semivariogram

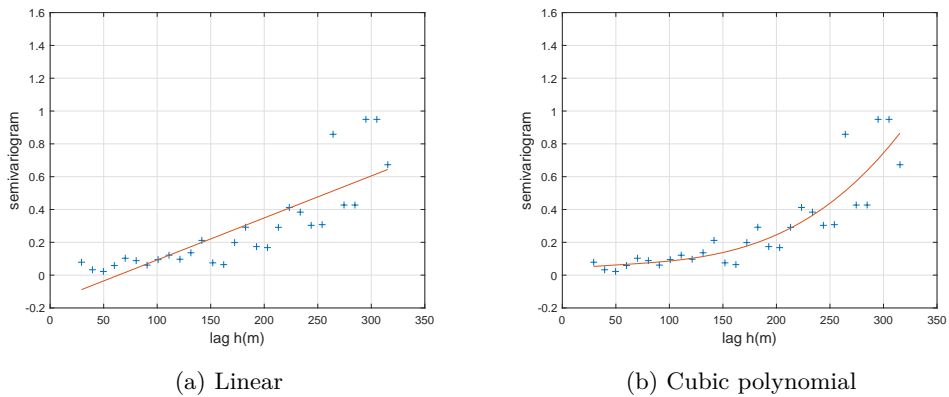


Figure 5: Mathematical model

Figure 4(a) shows the experimental semivariogram obtained from the basic 20 samples without Target A. From Figure 4(a), it is not clear to see the correlation between  $lag\ h$  and semivariogram. Figure 4(b) is the semivariogram obtained after applying the averaging processes mentioned in Section 5.2. The  $M = 28$  equal divi-



sions and the  $d = 10$  meters averaging radius at each division node were used. It is easy to see that Figure 4(b) shows clear correlation between  $lag\ h$  and semivariogram compared with Figure 2(a).

Figure 5 shows fitted mathematical models. The fitted linear model in Figure 5(a) was  $\gamma(h) = 0.0026h - 0.1632$ . Figure 5(b) shows the cubic polynomial model  $\gamma(h) = 3.83 \times 10^{-8}h^3 - 6.005 \times 10^{-6}h^2 + 0.0007h + 0.0364$ . The coefficients in the two models were estimated by the Least Square Optimization.

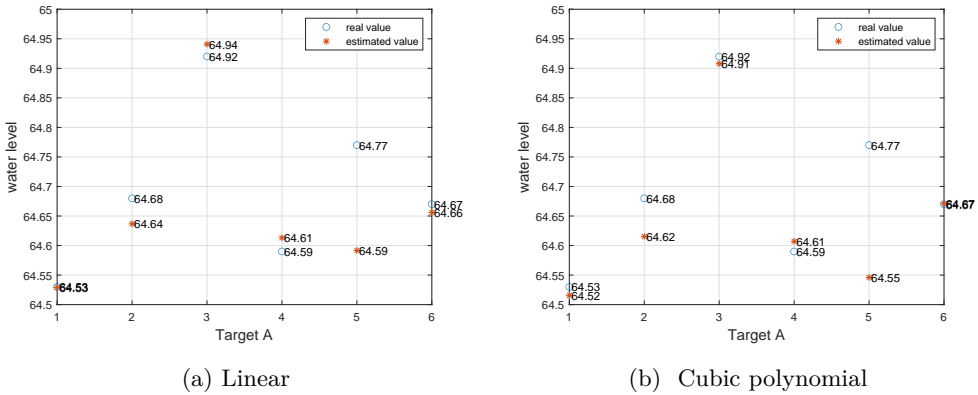


Figure 6: Estimation results for Target A

Table 2: Estimation results for each model

Linear model				Cubic polynomial model			
$R_v$	$E_v$	$ R_v - E_v $	$\sigma^2$	$R_v$	$E_v$	$ R_v - E_v $	$\sigma^2$
64.53	64.5290	0.0010	0.0533	64.53	64.5157	0.0143	0.0142
64.68	64.6367	0.0433	0.0530	64.68	64.6154	0.0646	0.0142
64.92	64.9409	0.0209	0.0540	64.92	64.9080	0.0120	0.0146
64.59	64.6131	0.0231	0.1026	64.59	64.6072	0.0172	0.0258
64.77	64.5918	0.1782	0.0692	64.77	64.5461	0.2239	0.0182
64.67	64.6560	0.0140	0.0976	64.67	64.6710	0.0010	0.0228

Figure 6 and Table 2 show the estimation results for Target A. In Table 2,  $R_v$  is the measured real value for Target A,  $E_v$  is the estimated value by kriging and  $\sigma^2$  is the kriging variance in (4.11). The averaged variances, the averaged  $|R_v - E_v|^2$ , for the linear and the cubic polynomial models were 0.0058 and 0.0092, respectively. The linear model could be better than the cubic polynomial one.

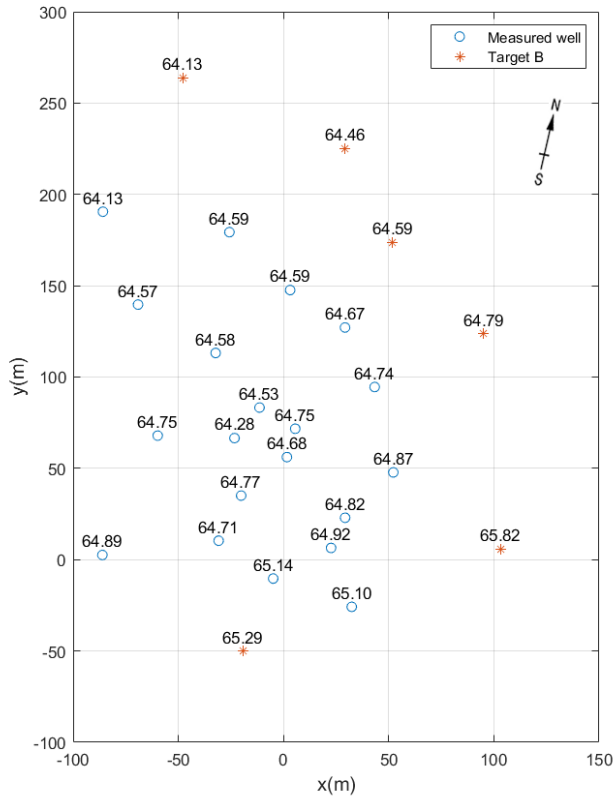


Figure 7: Water levels and Target B

To consider an extrapolation problem, six samples, Target B, located outside but near the boundary of the sampling network were selected. Target B is shown in Figure 7. Figure 8(a),(b) show experimental semivariogram and averaged semivariogram for

Target B, respectively. For Figure 8(b), the number of equal divisions  $M = 15$  and the averaging radius  $d = 15$  were selected.

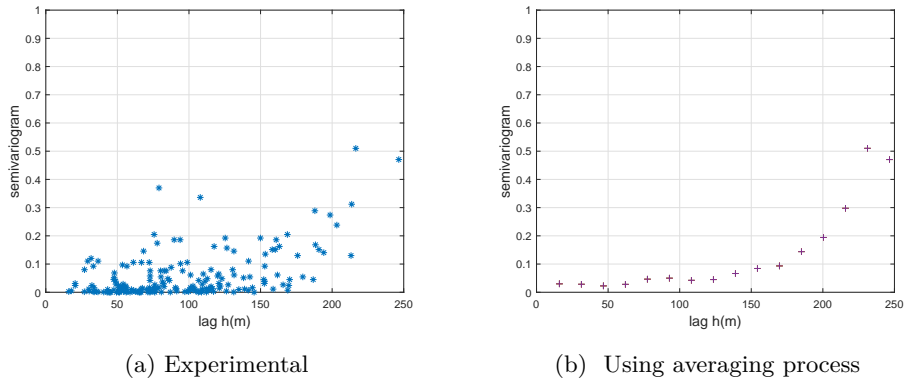


Figure 8: Semivariogram

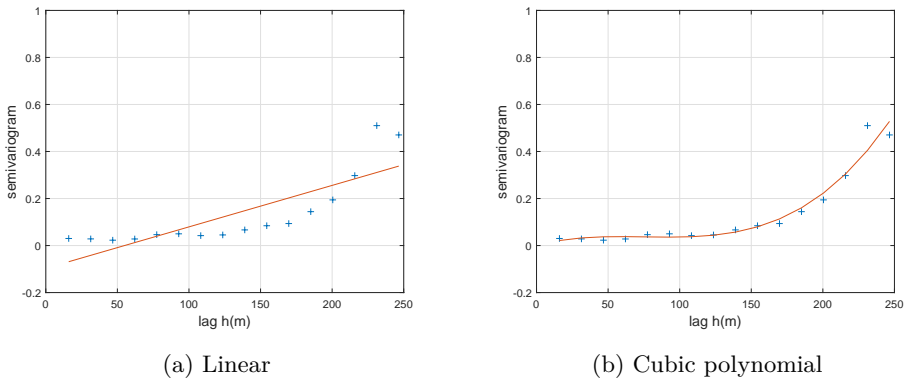
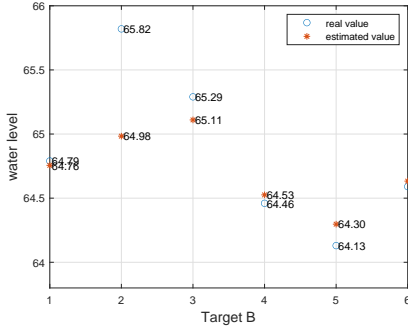


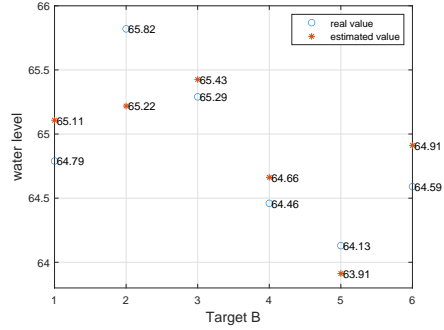
Figure 9: Mathematical model

Figure 9 shows a fitted mathematical models. In Figure 9, the linear mathematical model  $\gamma(h) = 0.0018h - 0.097$  and the cubic polynomial model  $\gamma(h) = 1.0082 \times 10^{-7}h^3 - 2.2757 \times 10^{-5}h^2 + 0.0016h + 0.0008$  were fitted.

Figure 10 and Table 3 show the estimation results for Target B. The averaged variance for the linear and the cubic polynomial models were 0.1279 and 0.1122, respectively.



(a) Linear



(b) Cubic polynomial

Figure 10: Estimation results for Target B

Table 3: Estimation results for each model

Linear model				Cubic polynomial model			
$R_v$	$E_v$	$ R_v - E_v $	$\sigma^2$	$R_v$	$E_v$	$ R_v - E_v $	$\sigma^2$
64.79	64.7558	0.0342	0.1687	64.79	65.1077	0.3177	-0.1033
65.82	64.9836	0.8364	0.1750	65.82	65.2184	0.6016	-1.0450
65.29	65.1101	0.1799	0.1118	65.29	65.4257	0.1357	0.1273
64.46	64.5256	0.0656	0.2076	64.46	64.6624	0.2024	-2.2141
64.13	64.2973	0.1673	0.2367	64.13	63.9122	0.2187	-4.4524
64.59	64.6330	0.0430	0.1399	64.59	64.9117	0.3217	0.0986

In Table 3, we notice that some of the kriging variance  $\sigma^2$  for the cubic polynomial model are negative. These phenomena are typical behaviors for extrapolation. In general, the estimated values for interpolation lie between the minimum and the maximum values of the sample values adopted for semivariogram. Therefore the kriging variance at each location becomes positive. On the other hand, the kriging variance for extrapolation need not be positive due to the fact that the estimated

value may be resided outside the selcected sample value range. Therefore, the kriging variance  $\sigma^2$  for extrapolation do not show much statistical meaning.

Figures 11 and 12 show the 3 dimensionanl mesh and their contour, respectively, for the surrounding domain including Table 1. We used all of 26 samples in Table 1.  $M = 15, d = 15$  were used for averaging process. The cubic polynomial model was fitted due to better performance. From Figures 11 and 12, it is easy to see that water flows from South-East to North-West. Recall that, as mentioned before, the positive y axis points in a direction 12 degrees West of true North.

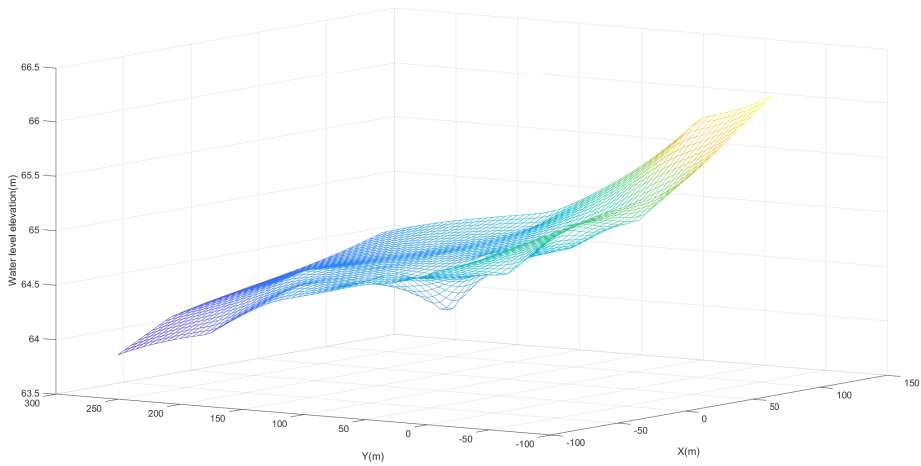


Figure 11: 3-D plot of the estimated water levels

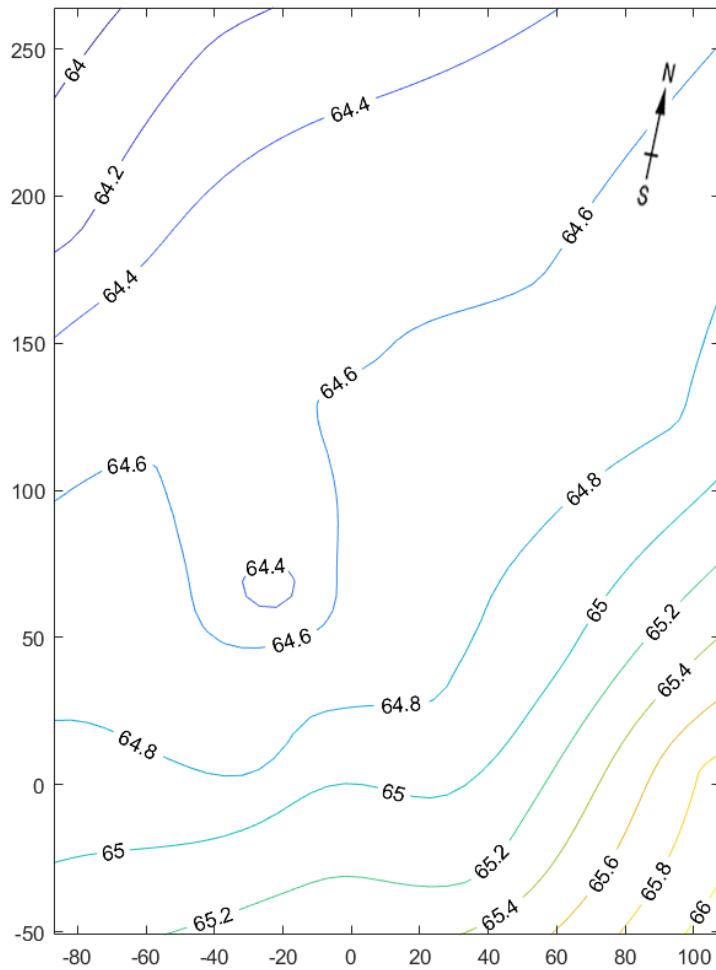


Figure 12: Contour of the estimated water levels

### 5.3.2 Example 2

The test site for Example 2 is located nearby the site in Example 1, see Figures 1 and 13. These tests were performed for investigating the hydraulic conductivities using the multi-level samples. The circles in Figure 13 are parts of well locations for Example 2. The total location and water tables are in Table 4.

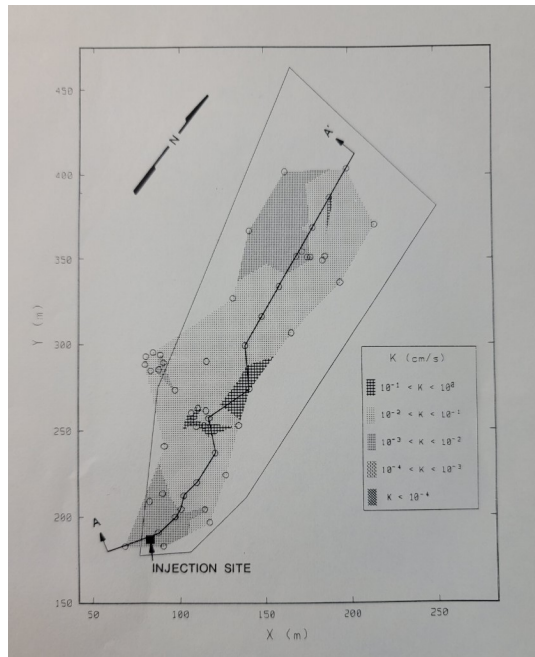


Figure 13: Sample site for Example 2

Water tables were measured at 66 locations. Among 66 samples, 16 locations, Target C, were selected for interpolation and 8 samples, Target D, were chosen for extrapolation. Figure 14 and Figure 21 show the interpolation and the extrapolation sampling networks, respectively. The positive direction in y axis in Figure 14 was adjusted so that it is parallel to true North.

For this example, conventional semivariogram, averaging process, spatial ratio, anisotropic aspects and combination of several semivariograms, etc., are applied.

Table 4: Water levels for Examle 2

Sample	$x(m)$	$y(m)$	$w(m)$	Sample	$x(m)$	$y(m)$	$w(m)$
W-1	69.945	-48.290	61.69	W-34	-16.245	104.513	63.16
W-2	75.226	-45.750	61.88	W-35	0.170	122.781	62.91
W-3	66.625	-57.631	61.54	W-36	21.572	141.017	63.06
W-4	43.014	-61.372	61.75	W-37	1.698	142.334	62.85
W-5	41.659	-37.024	62.00	W-38	38.332	219.812	63.12
W-6	-12.642	-12.292	61.63	W-39	3.432	162.520	62.82
W-7	7.112	-2.583	61.51	W-40	34.660	180.143	63.09
W-8	35.320	8.950	62.55	W-41	4.955	182.614	63.06
W-9	7.002	20.998	62.58	W-42	-26.306	184.260	63.12
W-10	25.458	21.384	61.39	W-43	6.391	202.379	63.09
W-11	19.487	26.902	61.39	W-44	7.911	222.572	63.09
W-12	5.173	28.518	61.57	W-45	9.535	242.871	63.06
W-13	-6.525	24.647	61.45	W-46	-22.613	224.994	63.06
W-14	-11.370	17.346	61.45	W-47	7.000	186.782	63.09
W-15	0.972	3.286	61.24	W-48	19.899	187.303	63.06
W-16	5.967	15.397	61.17	W-49	12.827	186.111	63.06
W-17	8.644	38.676	61.14	W-50	11.168	185.269	63.09
W-18	10.993	58.413	61.11	W-51	20.204	189.969	63.03
W-19	-0.842	75.225	61.17	W-52	13.254	100.878	63.16
W-20	-4.298	78.490	63.46	W-53	22.186	49.926	61.57
W-21	-9.004	77.825	63.37	W-54	-17.172	49.675	61.91
W-22	-11.430	73.707	63.43	W-55	16.599	79.084	61.69
W-23	-9.724	69.190	63.34	W-56	-10.820	11.040	62.36
W-24	-5.183	67.823	63.03	W-57	-6.020	9.270	62.33
W-25	-1.242	70.473	62.27	W-58	-0.680	7.240	62.36
W-26	-38.573	93.189	63.25	W-59	2.570	6.110	62.58



Sample	$x(m)$	$y(m)$	$w(m)$	Sample	$x(m)$	$y(m)$	$w(m)$
W-27	-41.984	96.453	63.28	W-60	5.500	5.040	62.48
W-28	-46.679	95.971	63.37	W-61	11.210	2.960	62.45
W-29	-49.259	91.990	63.43	W-62	-11.190	20.890	62.42
W-30	-47.639	87.421	63.43	W-63	-5.770	19.090	62.24
W-31	-43.033	85.874	63.49	W-64	-2.480	18.050	62.33
W-32	-39.086	88.349	63.49	W-65	2.060	16.290	62.42
W-33	-25.461	81.474	63.43	W-66	12.000	12.500	62.52



Figure 14: Well locations for Example 2 with Target C

First, we consider the interpolation problems with Target C. Figure 15 shows the experimental semivariogram and the improved semivariogram by applying averaging process and the fitted model with the improved semivariogram. The equal divisions  $M = 60$  and the averaging radius  $d = 5$  were chosen. The fitted exponential model is

$$\gamma_c(h) = c_0 + c_1 \left( 1 - \exp\left(-\frac{h}{c_2}\right) \right), \quad (5.1)$$

$c_0 = 0.2964$ ,  $c_1 = 0.5572$  and  $c_2 = 102.3438$ . The initial guess for the parameters  $c_0$ ,  $c_1$  and  $c_2$  were chosen as 0.1, 0.1, 100, respectively. The parameters in (5.1) were estimated by the nonlinear parameter estimation technique described in Section 3. Three iterations were enough for obtaining the final estimation.

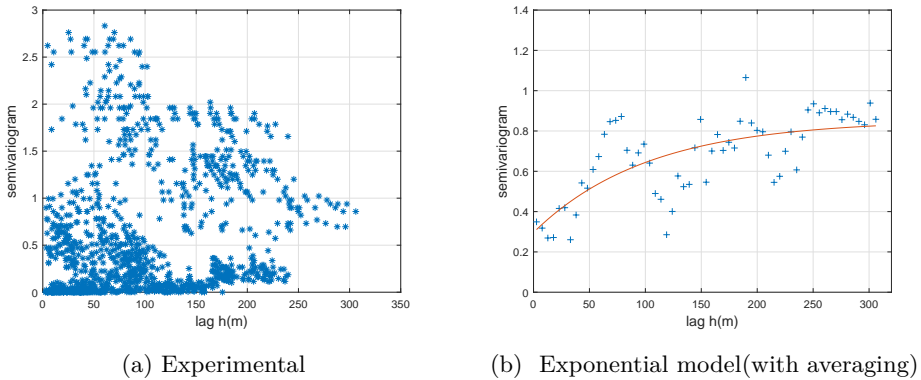


Figure 15: Semivariogram and exponential model

Figure 16 and Tabel 5 show the estimation results for Target C. The averaged  $|R_v - E_v|^2$  was 0.0261.

Next, we consider the combination of the conventional semivariogram with averaging process (Figures 15 and 16, Table 5) and the semivariogram obtained by accounting for anisotropic aspects (Figures 18 and 19, Table 6). To account for the directional aspects, we investigate the water table levels along each direction such as  $x$ -axis or  $y$ -axis (Figure 17). From Figure 17, it is easy to find a trend in  $y$ -axis.

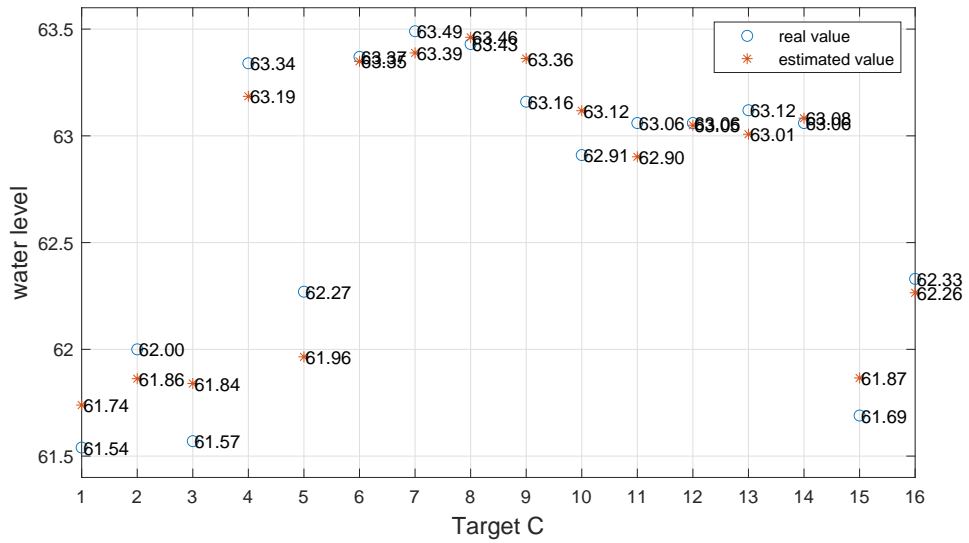


Figure 16: Estimation results for Target C

Table 5: Estimation results for Target C

$R_v$	$E_v$	$ R_v - E_v $	$\sigma^2$	$R_v$	$E_v$	$ R_v - E_v $	$\sigma^2$
61.54	61.7390	0.1990	0.0813	63.16	63.3621	0.2021	0.1265
62.00	61.8626	0.1374	0.1456	62.91	63.1178	0.2078	0.1163
61.57	61.8400	0.2700	0.0443	63.06	62.9019	0.1581	0.1383
63.34	63.1851	0.1549	0.0275	63.06	63.0498	0.0102	0.0395
62.27	61.9648	0.3052	0.0270	63.12	63.0076	0.1124	0.1908
63.37	63.3492	0.0208	0.0279	63.06	63.0827	0.0227	0.0160
63.49	63.3884	0.1016	0.0276	61.69	61.8660	0.1760	0.1014
63.43	63.4617	0.0317	0.0826	62.33	62.2649	0.0651	0.0281
$av = 0.0261$							

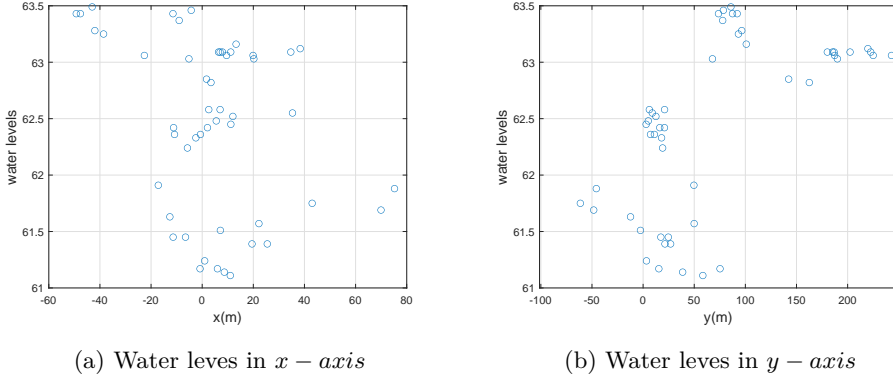


Figure 17: Water levels for Target C

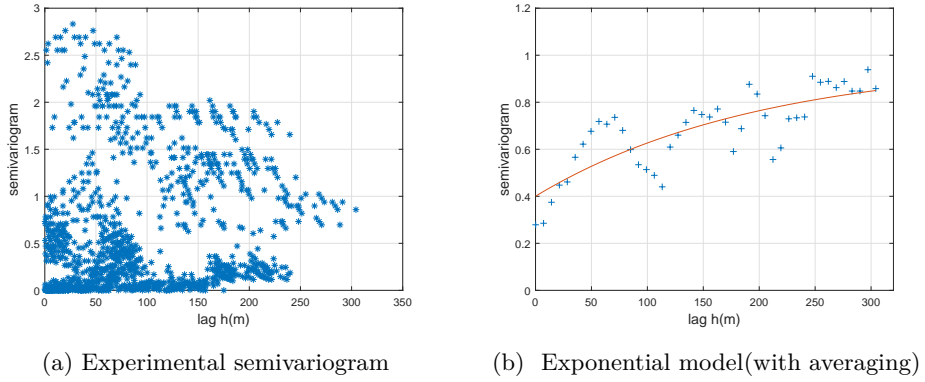


Figure 18: Semivariogram and exponential model (with y-direction)

Figure 18 shows the semivariogram accounted for the  $y$ -axis. For the averaging process  $M = 43, d = 7$  were chosen. The fitted exponential model becomes

$$\gamma_y(h) = c_0 + c_1 \left( 1 - \exp\left(-\frac{h}{c_2}\right) \right), \quad (5.2)$$

$c_0 = 0.4005, c_1 = 0.5751$  and  $c_2 = 200.0107$ . The final semivariogram for Target C was chosen as

$$\gamma = \gamma_c + \gamma_y, \quad (5.3)$$

where  $\gamma_c$  and  $\gamma_y$  are in (5.1) and (5.2), respectively.

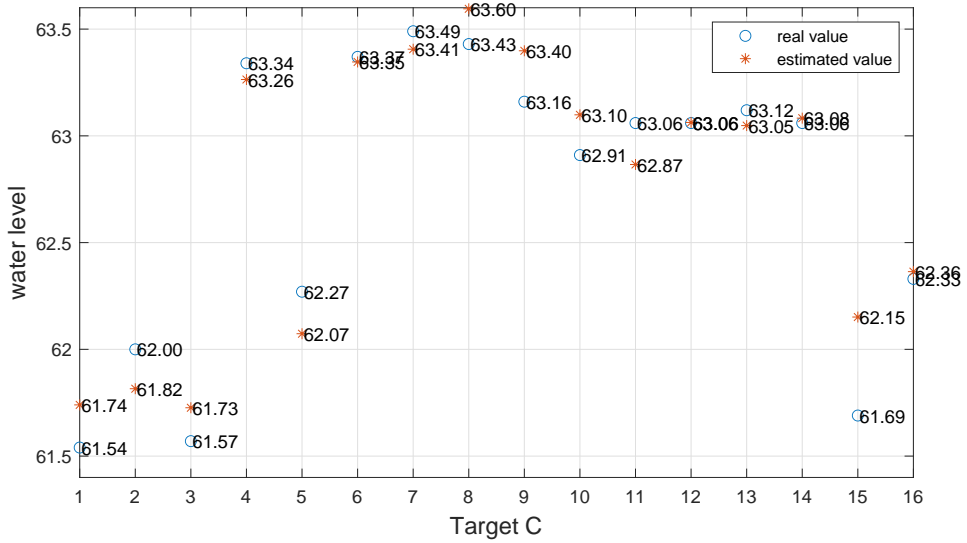


Figure 19: Estimation results for Target C with y-direction

The estimation results are shown in Figure 19 and Table 6. The averaged  $|R_v - E_v|^2$  was 0.0330.

Table 6: Estimation results for Target C with y-direction

$R_v$	$E_v$	$ R_v - E_v $	$\sigma^2$	$R_v$	$E_v$	$ R_v - E_v $	$\sigma^2$
61.54	61.7399	0.1999	0.1078	63.16	63.3985	0.2385	0.1578
62.00	61.8156	0.1844	0.2007	62.91	63.0986	0.1886	0.1761
61.57	61.7264	0.1564	0.0585	63.06	62.8659	0.1941	0.1608
63.34	63.2639	0.0761	0.0350	63.06	63.0628	0.0028	0.0546
62.27	62.0732	0.1968	0.0372	63.12	63.0481	0.0719	0.2309
63.37	63.3462	0.0238	0.0328	63.06	63.0830	0.0230	0.0190
63.49	63.4059	0.0841	0.0370	61.69	62.1513	0.4613	0.1243
63.43	63.5951	0.1651	0.0967	62.33	62.3640	0.0340	0.0337
$av = 0.0330$							

We now consider an extrapolation problem. Eight samples, Target D, were selected for the test as in Figure 20.

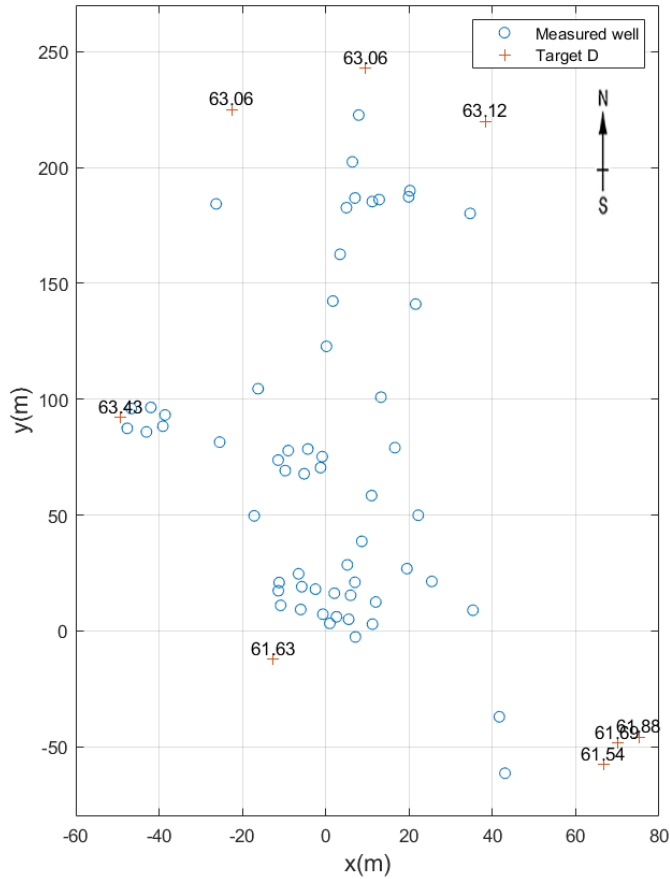


Figure 20: Well locations for Example 2 with TargetD

Figure 21 shows the experimental semivariogram and the improved semivariogram by applying averaging process and the fitted model with the improved semivariogram. For the averaging process, the equal divisions  $M = 28$  and averaging radius  $d = 10$  were chosen. The parameters in the fitted exponential model in (5.1) were  $c_0 = 0.3723$ ,  $c_1 = 0.5661$ ,  $c_2 = 199.1726$ .

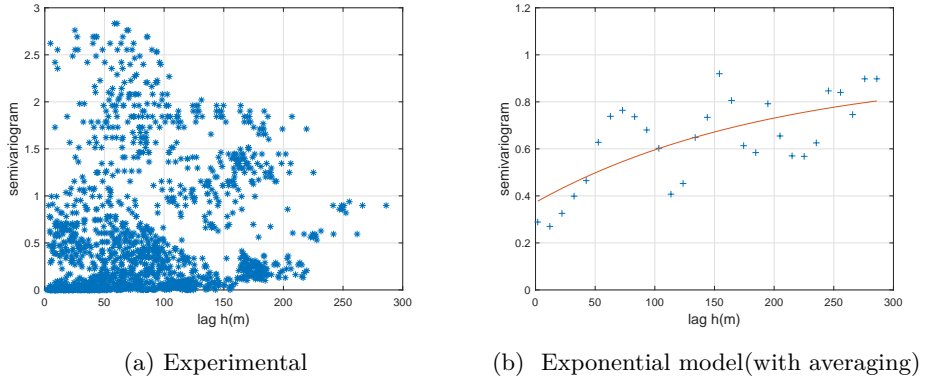


Figure 21: Semivariogram and exponential model

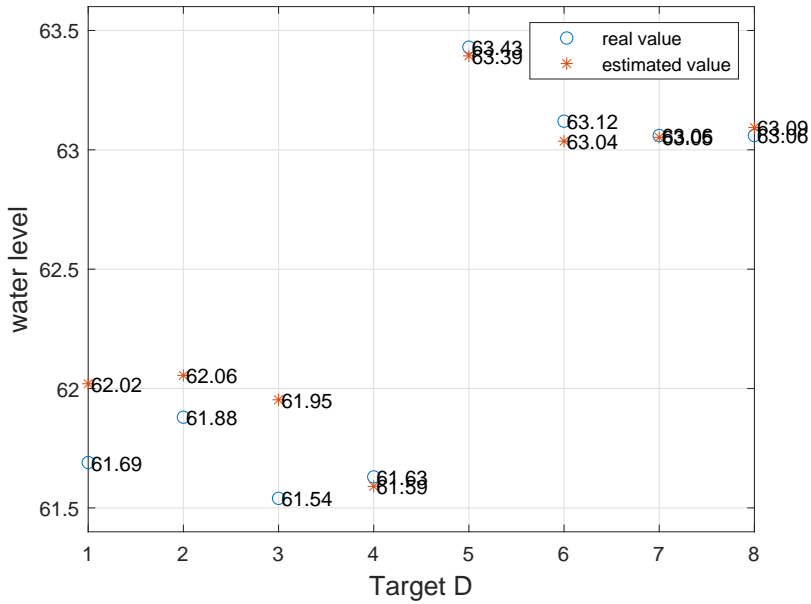


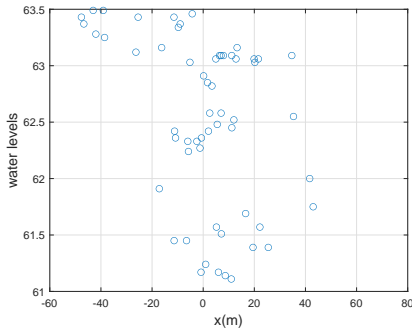
Figure 22: Estimation results for Target D

The estimation results are shown in Figure 22 and Tabel 7. The average variance is  $av = 0.0402$ .

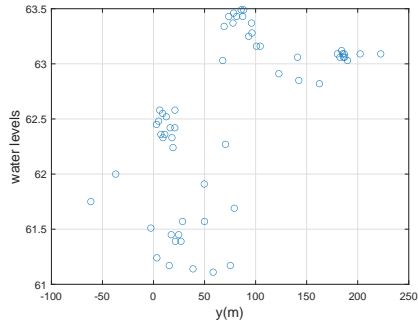
Figure 23 is for considering the anisotropic aspects. Those show that there is a clear tendency in  $y$ -direction.

Table 7: Estimation results for Target D

$R_v$	$E_v$	$ R_v - E_v $	$\sigma^2$	$R_v$	$E_v$	$ R_v - E_v $	$\sigma^2$
61.69	62.0201	0.3301	0.1203	63.43	63.3937	0.0363	0.0149
61.88	62.0551	0.1751	0.1409	63.12	63.0362	0.0838	0.1134
61.54	61.9530	0.4130	0.1095	63.06	63.0525	0.0075	0.1066
61.63	61.5902	0.0398	0.0810	63.06	63.0935	0.0335	0.1166
$av = 0.0402$							



(a) Water leves in  $x - axis$



(b) Water leves in  $y - axis$

Figure 23: Water levels for Target D

Figure 24 shows the semivariogram for the  $y$ -directional water level distribution. The equal divisions  $M = 26$  and averaging radius  $d = 11$  were chosen for the averaging process. The parameters of the optimized exponential model in (5.2) were  $c_0 = 0.4182$ ,  $c_1 = 0.5052$  and  $c_2 = 199.9545$ . The estimation results are shown in Figure 25 and Table 8. The average variance was  $av = 0.0270$ . From those, it is clear that the estimation results with consideration of  $y$ -direction are improved compared with the interpolation problem as shown in Figure 19 and Table 6. From this observation, consideration of anisotropic behavior on the sample set in Example 2 affects more on extrapolation than interpolation.



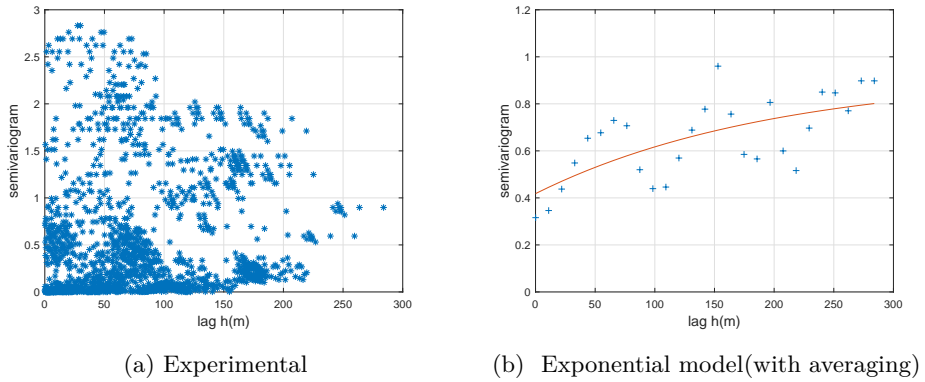


Figure 24: Semivariogram and exponential model (with y-direction)

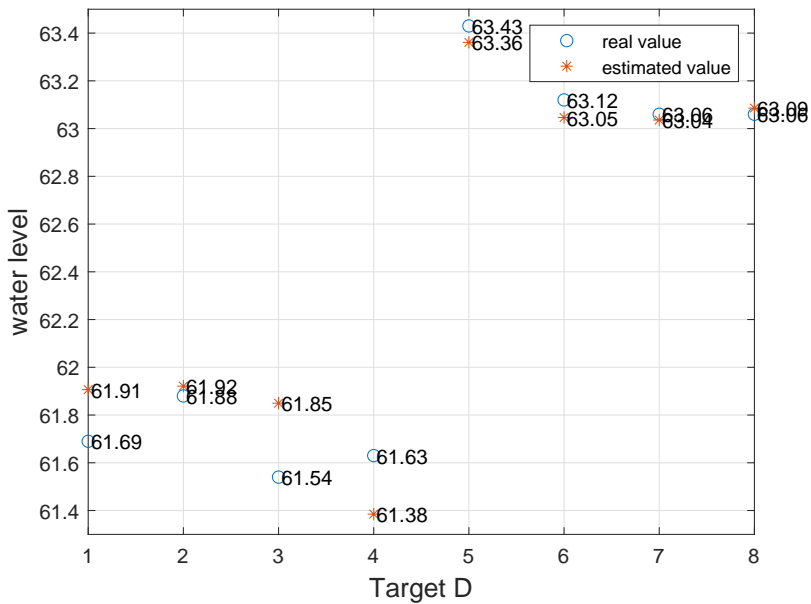


Figure 25: Estimation results for Target D with y-direction

In the following, the semivariogram with spatial ratio is considered for the extrapolation problem for Target D. Since the range of the sampling network is  $-47.639 \leq x \leq 43.014$  and  $-61.372 \leq y \leq 222.572$ , the approximate spatial distribution ratio is  $x : y \approx 1 : 3$ .

Table 8: Estimation results for Target D with y-direction

$R_v$	$E_v$	$ R_v - E_v $	$\sigma^2$	$R_v$	$E_v$	$ R_v - E_v $	$\sigma^2$
61.6900	61.9067	0.2167	0.1532	63.4300	63.3612	0.0688	0.0239
61.8800	61.9209	0.0409	0.1738	63.1200	63.0463	0.0737	0.1361
61.5400	61.8497	0.3097	0.1287	63.0600	63.0358	0.0242	0.2024
61.6300	61.3849	0.2451	0.1219	63.0600	63.0859	0.0259	0.1412
$av = 0.0270$							

The estimation results obtained by considering the spatial ratio are shown in Figures 26 and 27, Table 9.  $M = 29$  and  $d = 11$  were used for averaging process, and the fitted linear model in Figure 26 was  $\gamma(h) = 0.002h + 0.3169$ . The average variance was  $av = 0.0180$ .

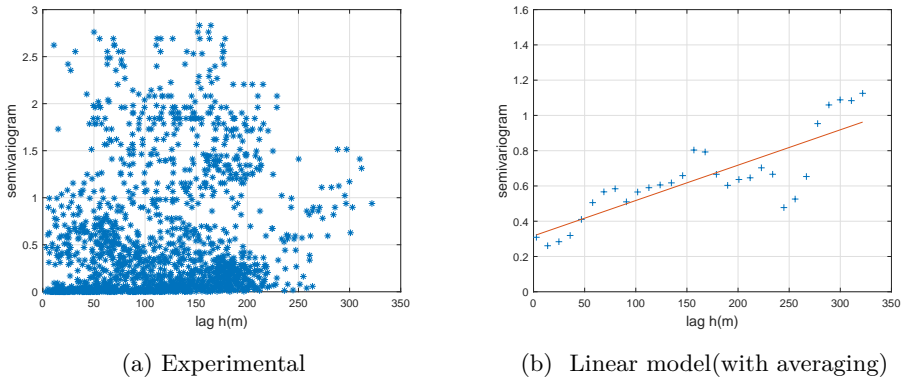


Figure 26: Semivariogram and Linear model (Target D ratio)

From Table 9 and Figure 27, we see that the extrapolation problem for Target D with spatial ratio are significantly improved. Specifically, the estimation variances for Target D with the conventional, the  $y$ -direction, and the spatial ratio were 0.0402, 0.0270 and 0.0180, respectively.

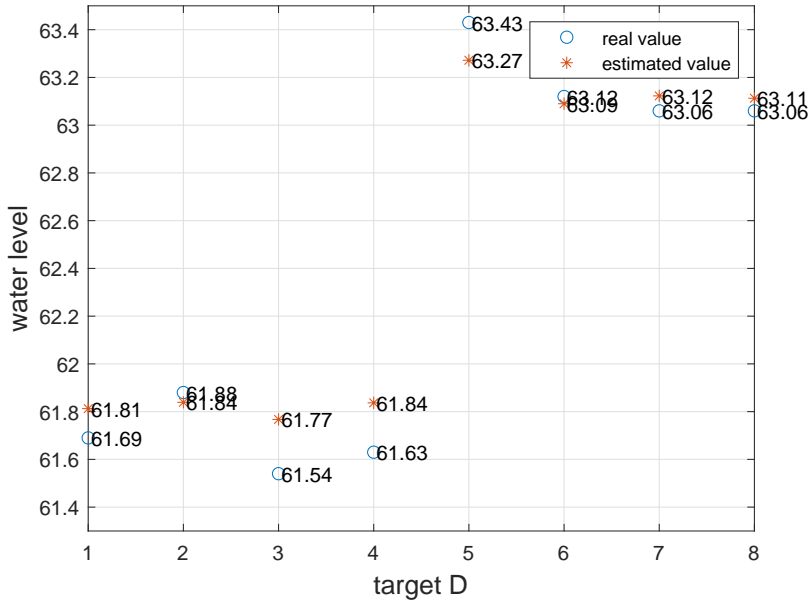


Figure 27: Estimation results for Target D with ratio

Table 9: Estimation results for Target D with ratio

$R_v$	$E_v$	$ R_v - E_v $	$\sigma^2$	$R_v$	$E_v$	$ R_v - E_v $	$\sigma^2$
61.6900	61.8126	0.1226	0.1186	63.4300	63.2719	0.1581	0.0309
61.8800	61.8389	0.0411	0.1108	63.1200	63.0898	0.0302	0.0432
61.5400	61.7674	0.2274	0.1345	63.0600	63.1227	0.0627	0.0902
61.6300	61.8368	0.2068	0.0564	63.0600	63.1127	0.0527	0.1111
$av = 0.018$							

Figures 28 and 29 are the three dimensional mesh and the contour plot for the sampling site for Example 2. For these plots, the semivariogram was obtained by considering the averaging process, the spatial direction, and the exponential model. The whole 66 measured samples (Table 4) were used for the construction of semi-

Table 10: Averaged  $|R_v - E_v|^2$  values for each problem

	Interpolation problem	Extrapolation problem
Averaging	0.0261	0.0402
Averaging, y-direction	0.0330	0.0270
Averaging, ratio	0.0875	0.0180

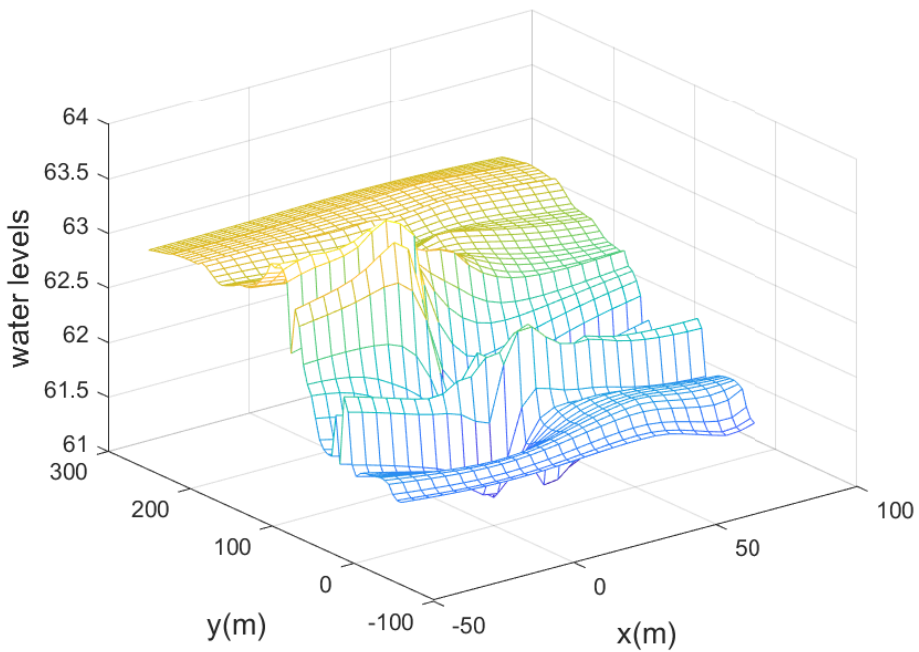


Figure 28: 3-D plot of the estimated water levels

variogram. These estimation process include interpolation as well as extrapolation problems, since the estimating locations lie in and out of the convex domain consisted of the given measured sampling network. From Figures 28 and 29, we can see that the water flows from North to South of the site.

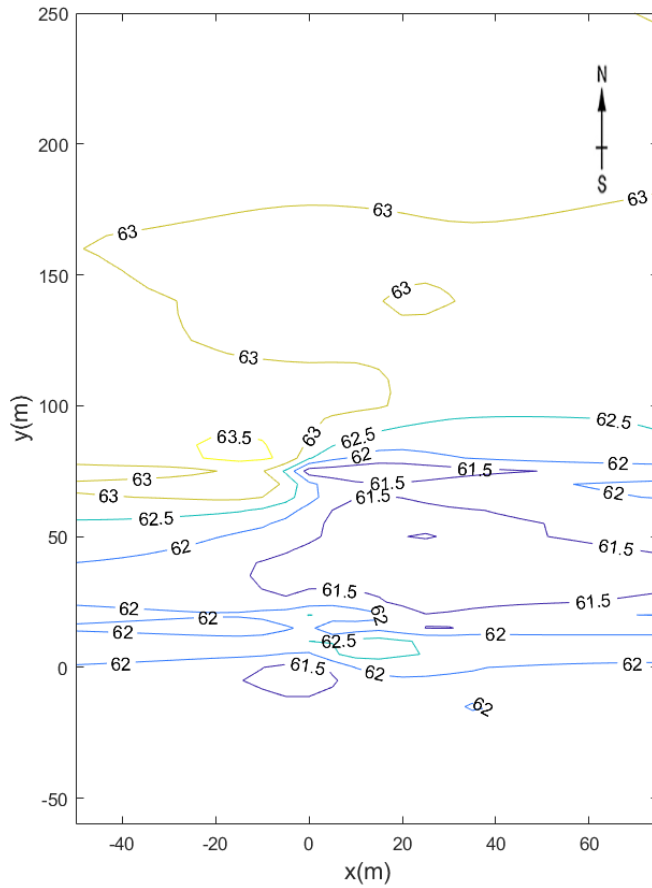


Figure 29: Contour of the estimated water levels

## 6. Conclusion

We considered interpolation and extrapolation problems for the in-situ groundwater tables. In general, extrapolations are known to be difficult to solve. The sample site is an alluvial aquifer. The aquifer is poorly-sorted to well-sorted sandy gravel and gravelly sand with minor amounts of silt and clay. Under the assumption that the geological properties of the site can be extended continuously to a larger region, the kriging system involving continuous averaging process, spatial ratio, and anisotropies produced accurate estimation results for extrapolation as well as interpolation problems. The kriging system considered in this paper can be applied for estimating groundwater levels of a continuously extendable alluvial aquifer.

## References

- [1] E. E. Adams and L. W. Gelhar, *Field study of dispersion in a heterogeneous aquifer, 2. Spatial moments analysis*, Water Resour. Res. 28(12) (1992) 3293- 3307.
- [2] ASCE Task Committe on Geostatistical Techniques in Geohydrology of the Ground Water Hydrology Committee of the ASCE Hydraulics Division, *Review of Geostatistics in Geohydrology. I. Basic concepts; II Applications*, Hydraulic Engineering 116, No. 5 (1990), 612-658.
- [3] J. M. Boggs and E. E. Adams, *Field study of dispersion in a heterogeneous aquifer, 4. Investigation of adsorption and sampling bias*, Water Resour. Res. 28(12) (1992), 3325-3336.
- [4] J. M. Boggs, L. M. Beard, W. R. Waldrop, T. B. Stauffer, W. G. MacIntyre, and C. P. Antworth, *Transport of tritium and four organic compounds during a natural gradient experiment (MADE-2)*, EPRI Report TR-101998, Electric Power Research Institute, Palo Alto, CA 94304, 1993.
- [5] J. M. Boggs, S. C. Young, L. M. Beard, L. W. Gelhar, K. R. Rehfeldt, and E. E. Adams, *Field study of dispersion in a heterogeneous aquifer, 1. Overview and site description*, Water Resour. Res. 28(12) (1992), 3281-3291.
- [6] J. M. Boggs, S. C. Young, D. J. Benton, Y. C. Chung, *Hydrogeologic Characterization of the MADE Site*, EN-6915, Research Project 2485-5, Tennessee Valley Authority Engineering Laboratory, July 1990
- [7] C. K. Cho and S. Kang, *A practical estimation method for groundwater level elevations*, J. Korean Math. Soc, 1997, 927-947.
- [8] Noel A. C. Cressie, *Statistics for Spatial Data*, John Wiley and Sons, Inc., New York, 1991.
- [9] J. C. Davis, *Statistics and Data Analysis in Geology*, John Wiley and Sons, New York, 1986.
- [10] R. Fletcher, *Practical Methods of Optimization, 2nd Ed.*, John Wiley and Sons, Chichester, 1993.

- [11] A. G. Journel and J. C. Huijbregts, *Mining Geostatistics*, Academic Press, San Diego, 1993.
- [12] D. G. Krige, *A statistical approach to some basic mine valuation problems on the Witwatersrand*, J. of the Chem., Metal. and Mining Soc. of South Africa. 52(6)(1951), 119–139.
- [13] J. H. Lee and S. Kang, *Complex nonlinear parameter estimation (CNPE) and obstacle shape reconstruction*, Computers and Mathematics with Applications 67 (2014), 1631-1642.
- [14] W. G. MacIntyre, J. M. Boggs, C. P. Antworth, and T. B. Stauffer, *Degradation kinetics of aromatic organic solutes introduced into a heterogeneous aquifer*, Water Resources Research 29(12) (1993), 4045-4051.
- [15] G. Matheron, *The theory of regionalized variable and its applications*, Les Cahiers du Centre de Morphologic Mathematique, Fasc. 5, CG Fontainebleau, 1971.
- [16] K. B. Mital, *Optimization Methods in Operations research and systems analysis*, Wiley Eastern Limited, 1976.
- [17] R. A. Olea, *Optimum Mapping Techniques Using Regionalized Variable Theory*, Kansas Geological Survey Series on Spatial Analysis No. 2 (1975).
- [18] Murray H. Protter and Charles B. Morrey Jr., *Intermediate Calculus (2nd ed.)*, Springer, New York, 1985.
- [19] K. R. Rehfeldt, J. M. Boggs, and L. W. Gelhar, *Field study of dispersion in a heterogeneous aquifer, 3. Geostatistical analysis of hydraulic conductivity*, Water Resour. Res. 28(12) (1992), 3309-3324.
- [20] T. B. Stauffer, et al., *Degradation of Aromatic Hydrocarbons in an Aquifer during a field Experiment Demonstrating The Feasibility of Remediation by Natural Attenuation*, AL/EQ-TR-1993-0007, Tennessee Valley Authority Engineering Laboratory and Environmentics directorate Tyndall AFB, April 1994
- [21] E.A. Varouchakis, D.T. Hristopulos, and G.P. Karatzas, *Improving kriging of groundwater level data using nonlinear normalizing transformations—a field application*, Hydrological Sciences Journal, 57(7) (2012), 1404-1419.



- [22] F. Yang, S. Cao, X. Liu, and K. Yang, *Design of Groundwater Level Monitoring Network with Ordinary Kriging*, J. of Hydrodynamics, Volume 20(2008), 339–346.